Research Article Available online www.ijsrr.org ISSN: 2279–0543

International Journal of Scientific Research and Reviews

AC Conductivity of Graphene Oxide Doped Titanium Dioxide Nanocomposite

Chikkappa Udagani[1*]

Department of Physics, University College of science, Tumkur University, Tumkur-572103 KNT India, E-mail: drchikkappa19@gmail.com

ABSTRACT

This paper demonstrates the synthesis of reduced graphene oxide doped titanium oxide (TiO_2/rGO) nanocomposite and AC conductivity of synthesized TiO_2 and TiO_2/rGO nanocomposite. The precipitation technique was used for the synthesis of TiO_2. TiO_2/rGO nanocomposite was prepared by mixing 10wt% of reduced graphene oxide with TiO_2 in isopropyl alcohol. The TiO_2 and TiO_2/rGO nanocomposite were characterized by XRD and SEM-EDAX. The characterization techniques reveal the successful synthesis of TiO_2 and TiO_2/rGO nanocomposite. The AC conductivity study was conducted using LCR meter UT612 at room temperature. From the AC conductivity measurement, dielectric constant, dielectric loss and ac conductivity of the TiO_2 and TiO_2/rGO nanocomposite are estimated.

KEY WORDS: DC conductivity, green synthesis, Four- probe technique, reduced graphene oxide, nanocomposite

*Corresponding author

Dr.Chikkappa Udagani

Department of Physics, University College of science,

Tumkur University, Tumkur-572103

Email: drchikkappa19@gmail.com

Mobile: 8050695873

INTRODUCTION

The graphene oxide (GO) is a 2-Dimensional carbon material and have single layer or multilayer structure [1]. GO is resultant of chemical exfoliation and oxidizing of layered crystalline graphite [2]. The GO found its application in graphene-based field effect transistor (FET) [3, 4]. The GO can be reduced through different reduction mechanisms namely electrochemical reduction, chemical reduction and thermal reduction.The GO and rGO can be used as electrode materials in batteries and double-layered capacitors, fuel cells and solar cells [5]. The rGO is useful as gas sensor against low concentration of pollutants such as NO_2 and NH_3 [6]. The TiO_2 can be used in variety of applications including photocatalysis, catalysis, dye sensitized solar cells, and photovoltaic devices [7]. The TiO_2 is a versatile material and it has number of applications in biomedical fields such as cosmetics, medicines and pharmaceutical products [8]. Because of wide band energy gap, TiO_2 shows poor electrical conductivity. The electrical conductivity of TiO_2 can be modified by the inclusion of rGO. The objective of the present work is to synthesize TiO_2/rGO nanocomposite and an attempt to understand the ac electric behaviour of TiO_2/rGO nanocomposite.

EXPERIMENTAL WORK

Titanium tetrachloride [$TiCl_4$], 20% ammonia solution, and commercially available reduced graphene oxide are used for synthesis of TiO_2 and TiO_2/rGO nanocomposite

Synthesis of Titanium Dioxide (TiO_2):

First 7ml of $TiCl_4$ was dissolved in 100ml of distilled water. Immediately 70ml of ethanol is added to the $TiCl_4$ solution in order to slowdown the reaction. Then a few drops of ammonia solution were added carefully using burette. After the addition of ammonia solution, milky $TiCl_4$ solution was turned into the white precipitate of TiO_2 nanoparticles. The precipitate was filtered and washed many times with distilled water. The filtered precipitate was initially oven dried at temperature 90^0C and then calcinated at the temperature 600^0C in the muffle furnace for 4 hours. The final product of TiO_2 nanoparticles was designated as TGN-0(0% rGO-100% TiO_2).

Synthesis of TiO_2/rGO nanocomposite:

20ml of isopropyl alcohol is taken in 100ml glass beaker. 0.134gm of rGO (10wt% of rGO relate to TiO_2) is added to 20ml isopropyl alcohol. The rGO- isopropyl mixture is stirred at 500rpm for 2 hours to get homogeneous mixture. After 2 hours 1.2 gm of TiO_2 is added to the rGO-isopropyl mixture. The stirring is continued at 350rpm until all the isopropyl alcohol is completely evoporated. It takes nearly 24 hours. The TiO_2/rGO nanocomposite is then oven dried at 100^0C to

remove moisture. The oven dried sample is grounded into fine powder using ultra clean agate mortar and pestle. The final product (10wt% rGO – 90wt% TiO_2) is labelled as TGN-10.

RESULTS AND DISCUSSION

X-Ray Diffraction Analysis

The phase purity of the samples was tested using X-ray diffractometer Bruker 8 Advance. The phase purity of the samples was tested using X-ray diffractometer Bruker 8 Advance. Figure (1) depicts the XRD pattern of rGO. The XRD peaks are observed at 2θ angles of 26.51, 54.63, 77.61 and 83.64conforming to the planes (1 1 1), (2 2 2), (-1 1 0) and (1 2 0) of rGO. The results are in agreement with the JCPDS card number 01-075-2078. The layer spacing (d – spacing) is calculated using Bragg's equation by considering the most intense XRD peak found at 2θ=26.55°. From the Bragg's equation the layer spacing is turned out to be 0.34nm.

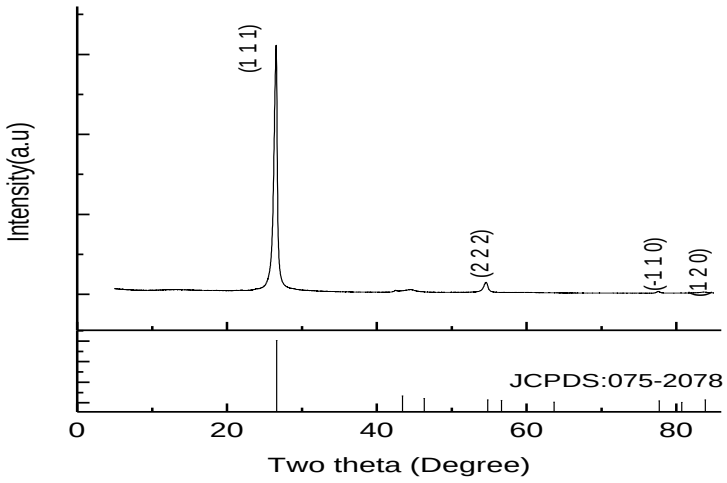

Figure (1): XRD pattern of rGO

Figure (2) depicts the XRD pattern of TGN-0. The figure illustrates the intense XRD peaks at 2θ angles of 27.447, 36.086, 39.188, 41.226,54.32, 62.74, 64.04, 69.01, 69.7, 72.41,76.51, 79.82 and 84.26 The sharp XRD peaks illustrate the crystalline nature of the synthesized TiO2 nanoparticles. No impurity peaks other than TiO_2 are observed in the XRD pattern which indicates the high phase purity of the synthesized TiO2. The XRD peaks at 2θ angles of 27.57, 36.20, 39.30, 41.38, 44.17, 54.35, 56.74, 62.76, 64.17, 69.18, 69.97, 76.78, 79.99 and 82.41 are consistent with JCPDS card number 00-021-1276 and indexed for crystal planes (1 1 0), (1 0 1), (2 0 0), (1 1 1), (2 1 0) (2 1 1), (2 2 0), (0 0 2), (3 1 0), (3 0 1),

(1 1 2), (2 0 2), (2 1 2) and (3 2 1) respectively corresponding to hexagonal TiO_2 with lattice parameters: a: 4.5933 Å and c: 5.9592 Å.

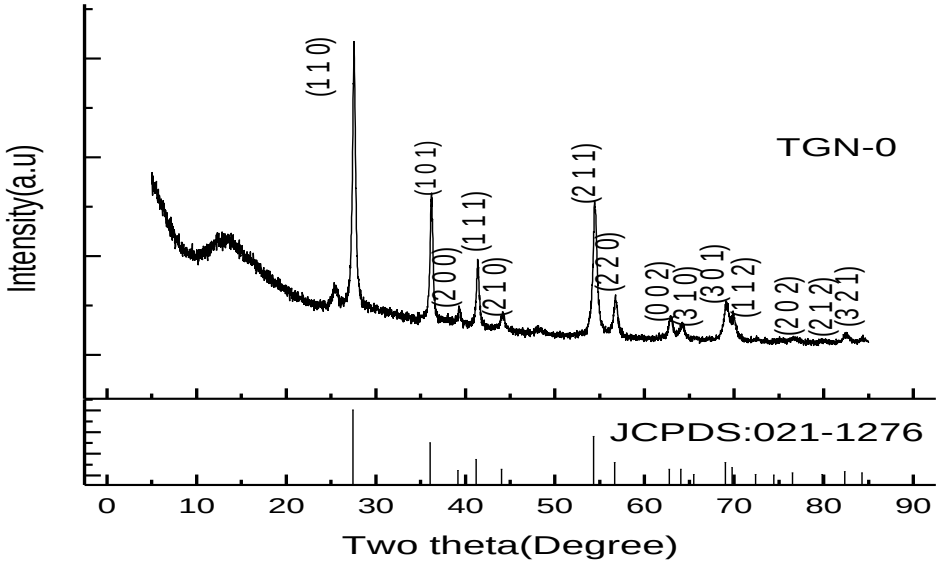

Figure (2): XRD pattern of TGN-0

The XRD pattern for TiO_2/rGO nanocomposite, TGN-10 is illustrated in the Figure (3). In the case of TGN-10 all the TiO_2 peaks are reappeared. In addition to TiO_2 peaks, the XRD peak due to reflection (1 1 1) is present in the sample TGN-10. This is due to inclusion of rGO in the lattice of TiO_2.

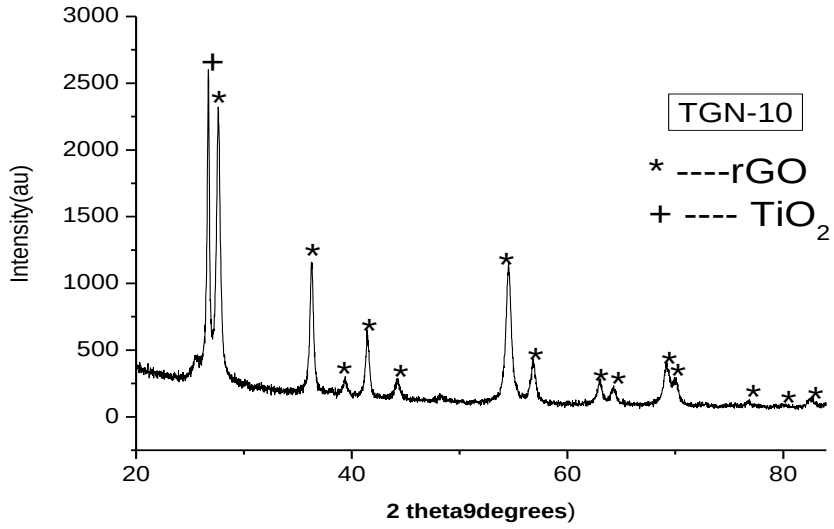

Figure (3): XRD pattern of TGN-10

The crystallite size was found from substituting the value of β in the Scherrer` equation:

$$D = \frac{K \times \lambda}{\beta \times \cos\theta}$$

Where, D- Average crystallite size (nm); K - Scherrer constant. K varies from 0.68 to 2.08. K=0.94 for spherical crystallites with cubic symmetry; λ- X ray wavelength; β- FWHM (Full width half maximm) of XRD. The Full width at half maximum (β) was estimated using Fityk software[10]. The Figures (4) & (5) show the Fityk analysis for TGN-0 and TGN-10.

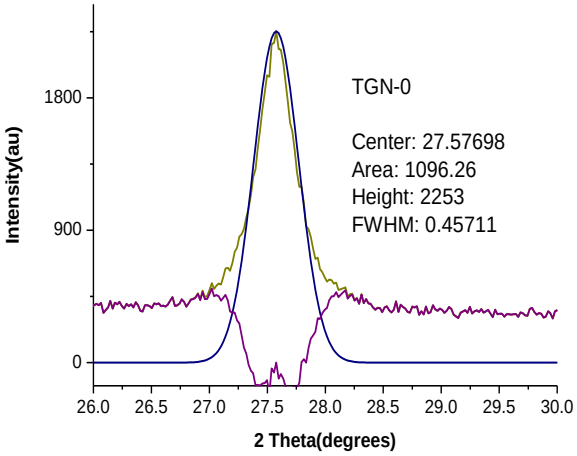

Figure (4): Fityk analysis for TGN-0

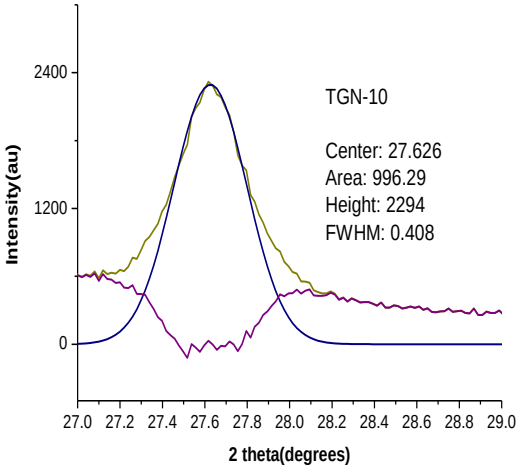

Figure (5): Fityk analysis for TGN-10

From the FityK analysis it is found that the crystallite size of TGN-0 is estimated to be 25.85nm. For TGN-10, the crystallite size is turn out turn - out to be 27.47nm. From the analysis it is also evident that, the crystallite size of the TGN-10 is greater than that of TGN-0. This can be attributed to the inclusion of rGO in the crystal lattice of TiO_2.

SEM-EDAX:

The SEM micrograph of TGN-0 is shown in the Figure (6). The SEM micrograph of and TGN-0 shows the spherical morphology of the nanoparticles and it shows that the nanoparticles are distributed uniformly in the space. The Figure (7) depicts the SEM micrograph of TGN-10. The the SEM micrograph of TGN-10 shows the inclusion of rGO with the TiO_2 nanoparticles.

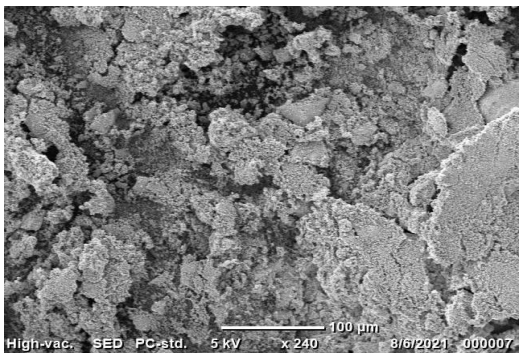

Figure (6): SEM micrographs of TGN-0.

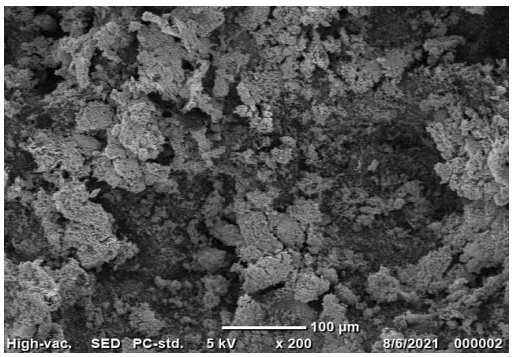

Figure (7): SEM micrographs of TGN-10

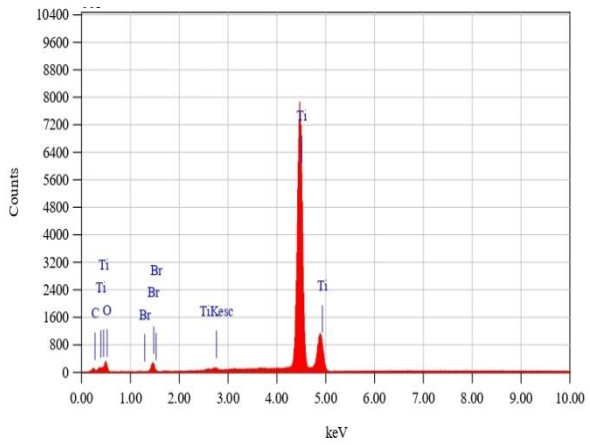

Figure (8): EDAX of TGN-0

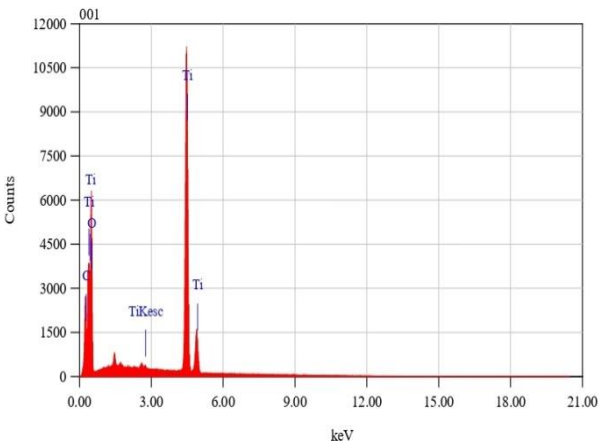

Figure (9): EDAX of TGN-10

The Figure (8) depicts the EDAX of TGN-0. From the Figure it is seen the sharp peaks of Ti and O. This illustrates the successful synthesis of TiO_2 nanoparticles. The Figure (9) depicts the EDAX of TGN-10. The presence of C, Ti and O peaks in the EDAX of the TGN-10 indicates the effective synthesis of TiO_2/rGO nanocomposite.

AC CONDUCTIVITY STUDY:

The fine powder of TiO_2 and TiO_2/rGO nanocomposite were pelletized using hydraulic press at a pressure of around 2 ton. The pellets were allowed to dry at room temperature for 15 days to completely remove the moisture. The pellets were then polished smoothly using sand paper for effective electrical contact. The ac measurements were carried out using LCR meter UT612. The Figures (10) & (11) show the frequency dependence of dielectric constant, $\boldsymbol{\varepsilon'}$ of the TGN-0 and TGN-10. The dielectric constant, $\boldsymbol{\varepsilon'}$ decreases with increasing frequency for the samples. The dielectric constant TGN-10 is greater than that of the TGN-0 which means that the TGN-10 is found to be more efficient for storing electric energy than the TGN-0.

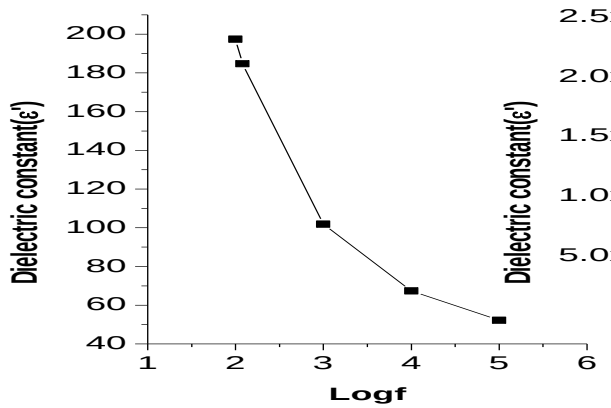

Figure.10: Plot of dielectric constant versus logf for TGN-0

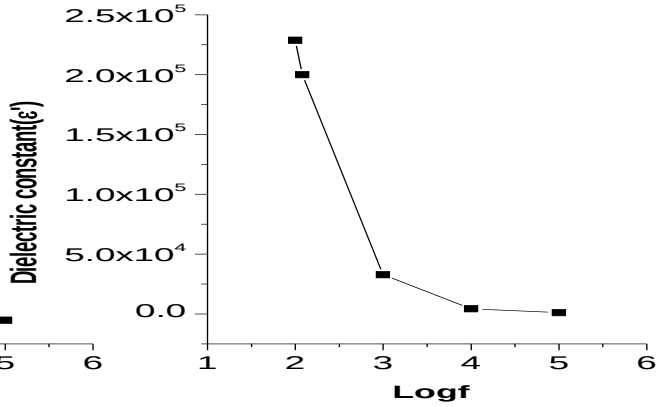

Figure.11: Plot of dielectric constant versus logf for TGN-10

The Figures (12) & (13) depict the frequency dependence of dielectric loss, **ε″** of the TGN-0 and TGN-10. The dielectric loss **ε″** signifies the energy dissipation in dielectric material when the material is subjected to an ac signal. The dielectric loss **ε″** varies inversely with applied frequency. It is also found that, TGN-10 has greater dielectric loss than the TGN-0.

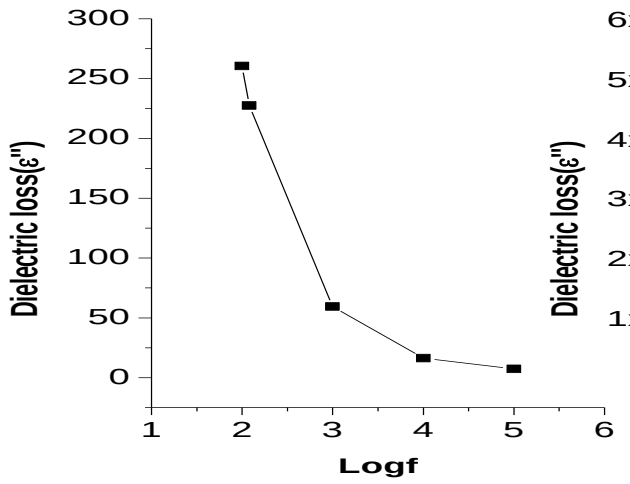

Figure.12: Plot of dielectric loss versus logf for TGN-0

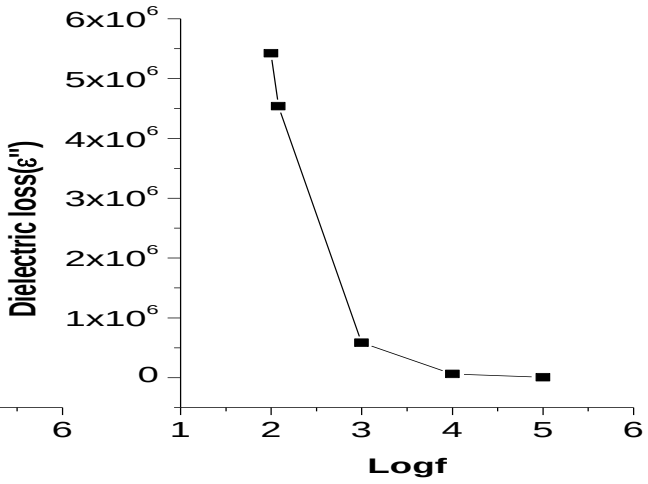

Figure.13: Plot of dielectric loss versus logf for TGN-10

The Figures (14) & (15) depict the frequency dependence of ac conductivity. The ac conductivity of TGN-0 increases with increasing frequency of the applied voltage. This is also true for TGN-10. This increase in ac conductivity with frequency may be attributed to increase in charge carriers hopping in the sample with frequency. It is also evident that ac conductivity of TGN-10is higher compared to TGN-0 because of availability of free electrons for electric conduction.

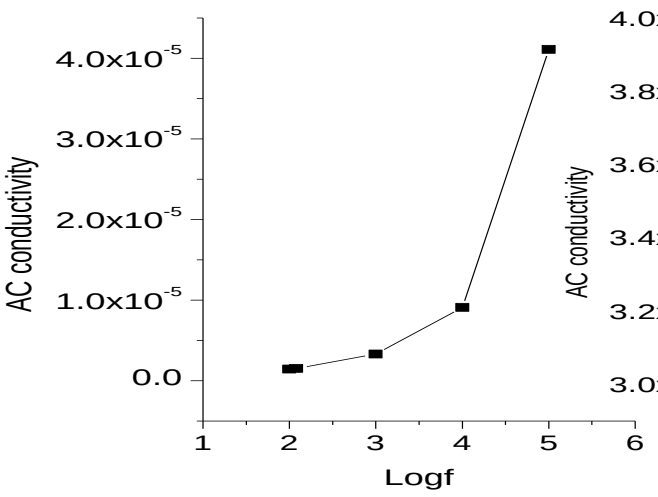

Figure.14: Plot of ac conductivity versus logf for TGN-0

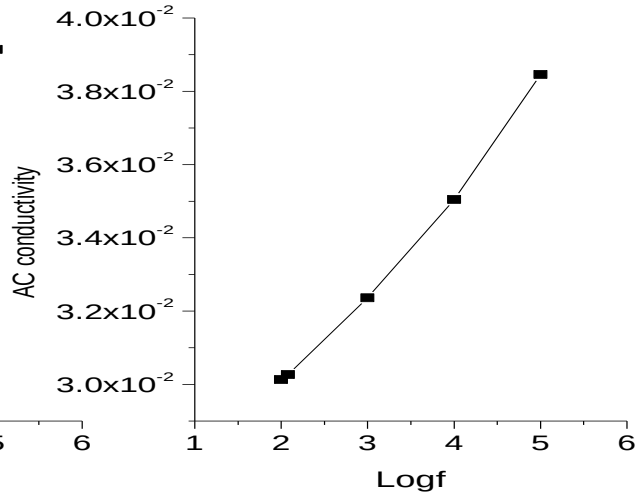

Figure.15: Plot of ac conductivity versus logf for TGN-10

CONCLUSION

The TiO_2 (TGN-0) and TiO_2/rGO (TGN-10) nanocomposite were more effectively synthesized. The synthesized samples have been characterized using XRD and SEM-EDAX. The XRD analysis confirms the high purity and crystalline nature of TiO_2. The Fityk analysis of the XRD data shows that the synthesized samples are of nano size. The XRD analysis of TiO_2/rGO (TGN-10) nanocomposite illustrates the successful blending of TiO_2NPs in rGO. The blending of TiO_2 in rGO can be visualized by SEM image of TiO_2/rGO (TGN-10) nanocomposite. This result is further supported by EDAX of TiO_2/rGO (TGN-10) nanocomposite. The ac conductivity measurement shows the increasing trend of ac conductivity with frequency of ac signal for TiO_2 (TGN-0) and TiO_2/rGO (TGN-10) nanocomposite. The dielectric study shows decreasing trend of both dielectric constant and dielectric loss with frequency for both the samples. In the lower frequency range there may be faster response of dipoles to the frequency of the applied field and dipole polarization has maximum value. At higher frequencies of the order of 10^4 kHz, dipole polarizability will reach minimum value due to poor response of dipoles to the frequency of the applied field. Therefore dielectric values; dielectric constant and dielectric loss saturate at minimum value. From this one can conclude that ac conductivity, dielectric constant and dielectric loss of TiO_2 can be moulded according to our need by proper blending of rGO in the lattice of TiO_2.

REFERENCES

1. Bianco A, Cheng H, Enoki T, Gogotsi Y, Hurt R, Koratkar N, Kyotani T, Monthioux M., Park C, Tascon J. and Zhang J. All in the graphene family – A recommended nomenclature for two-dimensional carbon materials, Carbon 2013; 65: 1-6.
2. Park S, Ruoff R Erratum. Chemical methods for the production of graphenes, Nature Nanotechnology 2010; 5:309-309.
3. Su C, Xu Y, Zhang W, Zhao J, Liu A, Tang X et al. Highly Efficient Restoration of Graphitic Structure in Graphene Oxide Using Alcohol Vapors. ACS Nano. 2010; 4(9):5285-5292.
4. Wang S, Ang P, Wang Z, Tang A, Thong J, Loh K. High Mobility, Printable, and Solution-Processed Graphene Electronics. Nano Letters. 2009;10(1):92-98.
5. Zhu Y, Murali S, Cai W, Li X, Suk J, Potts J, Ruoff R. Graphene and Graphene Oxide: Synthesis, Properties, and Applications, Advanced Materials 2010; 22:3906-3924
6. Lu G, Park S, Yu K, Ruoff RS, Ocola LE, Rosenmann D, Chen J. Toward Practical Gas Sensing with Highly Reduced Graphene Oxide: A New Signal Processing Method To Circumvent Run-to-Run and Device-to-Device Variations. ACS Nano. 2011;5(2):1154-1164.

7. Fujishima A, Zhang X. Titanium dioxide photocatalysis: present situation and future approaches. Comptes Rendus Chimie. 2006; 9(5-6):750-760.
8. Garimella R, Eltorai A. Nanotechnology in orthopedics. Journal of Orthopaedics. 2017; 14(1):30-33.
9. Wojdyr M. Fityk: a general-purpose peak fitting program. Journal of Applied Crystallography. 2010; 43(5):1126-1128.